Supplemental Information

Supplemental materials and methods

Generation of tamoxifen-inducible *Col7a1* knockout mouse and wound healing studies

The *Col7a1*-hypomorphic mouse line has been described previously (22). Briefly, a construct with two loxP sites flanking exon 2 and Neo cassette surrounded by two FRT sites was inserted by homologous recombination, termed *Col7a1*$^{fl/neo}$allele. The presence of the Neo cassette downstream exon 2 led to abnormal *Col7a1* splicing and subsequently reduces COL7A1 expression. The above construct was used to create a tamoxifen-inducible *Col7a1* knockout mouse. First, the Neo cassette was removed after homologous recombination and selection using FLP-FRT recombination, resulting in a *Co7a1*^{fl}allele. Homozygous *Col7a1*$^{fl/fl}$ mice are phenotypically indistinguishable from wild-type littermates and fertile. Second, to generate a tamoxifen-inducible knockout, the mice were crossed with B6.Cg-Tg(CAG-cre/Esr1*)5Amc/J strain (Jackson laboratory, Bar Harbor, ME), which carries tamoxifen-inducible Cre driven by the chicken beta actin promoter/enhancer coupled with the cytomegalovirus (CMV) immediate-early enhancer (Supplemental Figure S3A). The Cre-loxP recombination, initiated by administration of tamoxifen, removes exon 2, which creates a premature stop codon after 42 amino acids, thus terminating COL7A1 expression. Efficient recombination with subsequent reduction of COL7A1 expression after tamoxifen treatment was verified by analyzing cells isolated from mice homozygous for *Col7a1*^{fl} and carrying Cre (Supplemental Figure S3, B and C). Mice were genotyped for WT or *Co7a1*^{fl} alleles as previously described (22) and for Cre using primers: Cre forward 5' gacggaaatccatcgctcgaccag3' Cre reverse 5' gacatgttcagggatcgccaggcg 3'.

For the wound healing studies, 4-6-week-old homozygous tamoxifen-inducible COL7A1 knockout mice positive or negative for Cre expression were used. *Col7a1* deletion was initiated by daily intraperitoneal injections of 40 µg tamoxifen (Sigma-Aldrich) / g body weight for five consecutive days. Control mice negative for Cre expression received the same

treatment. The mice were allowed to recover for 9 days after the last tamoxfien treatment before wounding. The wound healing experiments were performed as described for the *Col7a1*-hypomorphic mouse (see Materials and methods, Assessment of wound healing).

Supplemental figures and figure legends

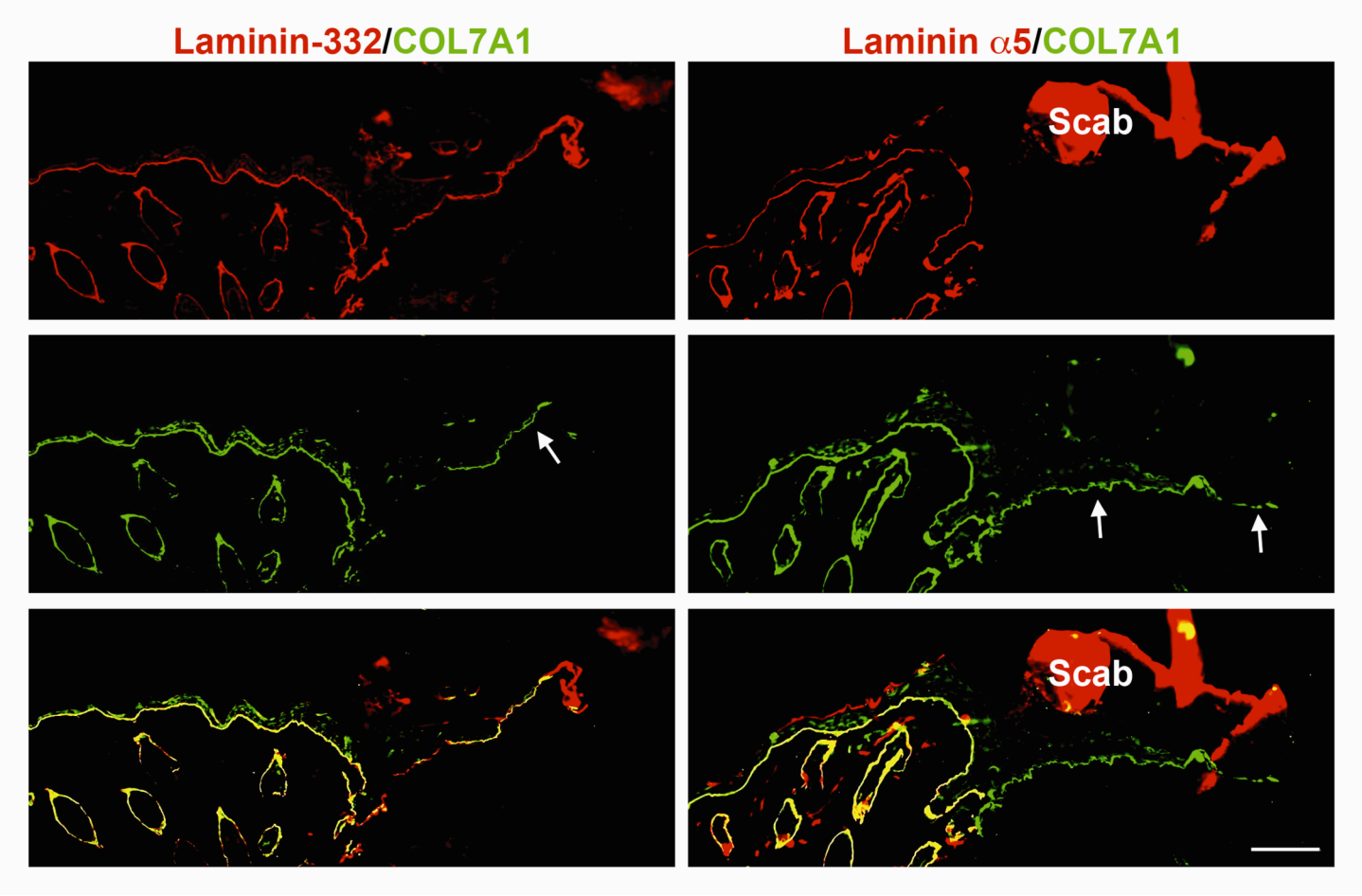

Supplemental Figure 1. In wild-type wounds, COL7A1 is expressed and deposited under the epidermal tongue. The epidermal tongue at day 3 after wounding was stained for COL7A1 (green) and laminin-332 (red) or laminin α5 (red) as indicated; bar = 50 μm. Laminin-332 is deposited by migrating keratinocytes (55), whereas laminin α5 is only part of the mature dermal-epidermal basement membrane. Hence, COL7A1 is present early on in the provisional DEJZ during wound healing. Arrows point to COL7A1 deposition under the epidermal tongue.

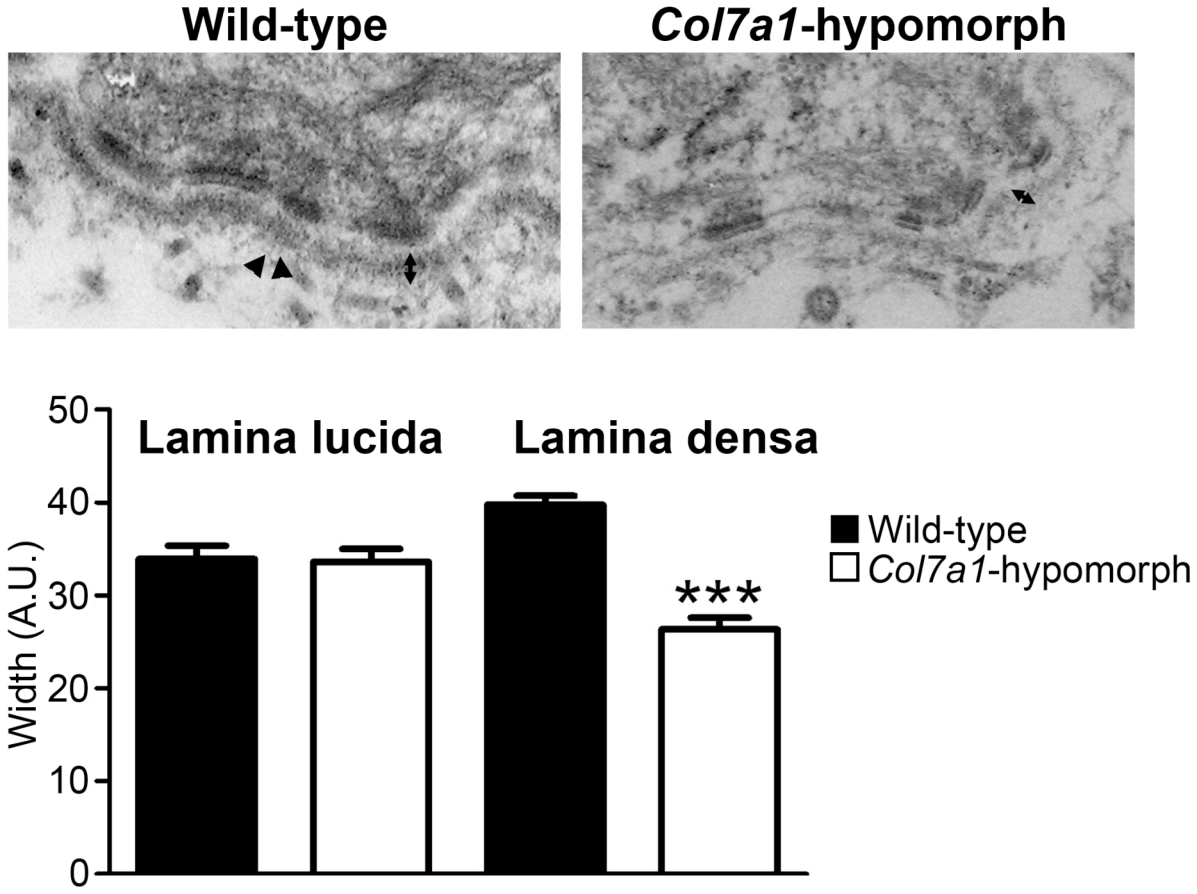

Supplemental Figure 2. Ultrastructural analysis of the dermal-epidermal basement membrane zone in COL7A1-deficient skin. The images generated from transmission electron microscopic analysis of skin from adult wild-type and *Col7a1*-hypomorphic littermates as indicated. Double-headed arrows show the lamina densa and arrowheads point to anchoring fibrils. Original magnification 39,000X. The bar graph shows the quantification of the width of lamina lucida and lamina densa in 12 randomly selected electron micrographs from 4 different mice. Values in the bar graph represent mean ± S.E.M. ***p<0.001; bar = 50 μm.

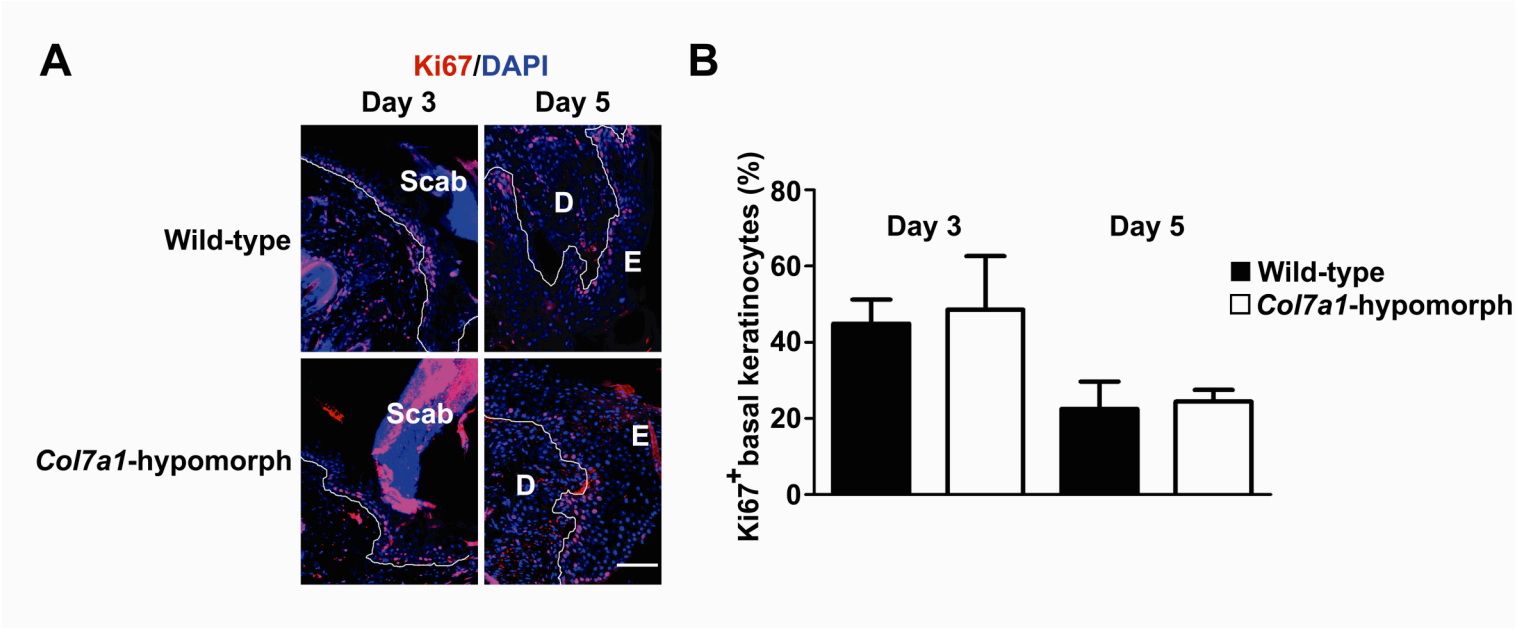

Supplemental Figure 3. Loss of COL7A1 does not alter keratinocyte proliferation during wound healing. **A,** Ki67 (red) and DAPI (blue) staining of wound margins of 3- and 5-day-old wild-type and *Col7a1*-hypomorphic wounds. White lines mark the dermal-epidermal junction. E indicates epidermis and D dermis. Bar = 50 μm. **B,** Quantification of Ki67 positive basal keratinocytes as in panel **A**. Values represents mean ± S.E.M; n ≥ 3 wounds per day and genotype.

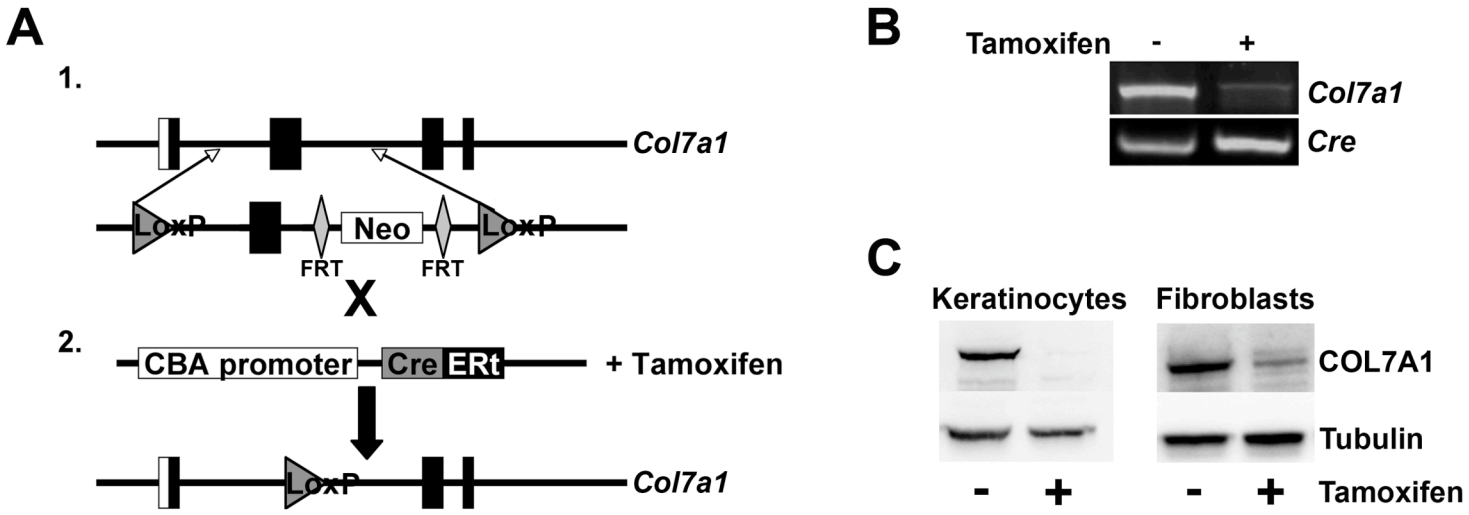

Supplemental Figure 4. Tamoxifen-inducible *Col7a1* knockout mouse model. **A**, Schematic representation of the knockout construct. Lox-P sites were inserted flanking exon 2 in the *Col7a1* gene. Mice carrying this transgene were crossed with mice expressing tamoxifen activating Cre under the chicken beta actin (CBA) promoter. Activation of Cre by tamoxifen leads to removal of exon 2 and creates a pre-mature stop codon after 42 codons, thus terminating COL7A1 expression. **B**, Verification of the knockout; dermal fibroblasts treated ± 1µM 4-OH tamoxifen. PCR of genomic DNA with primers placed up- and downstream of the first Lox-P site and exon 2, respectively, Cre treated with vehicle (DMSO) was used as control. **C**, Western blots confirming loss of COL7A1 in both keratinocytes and fibroblasts after treatment with 1µM tamoxifen for 10 days (keratinocytes) and 5 days (fibroblasts).

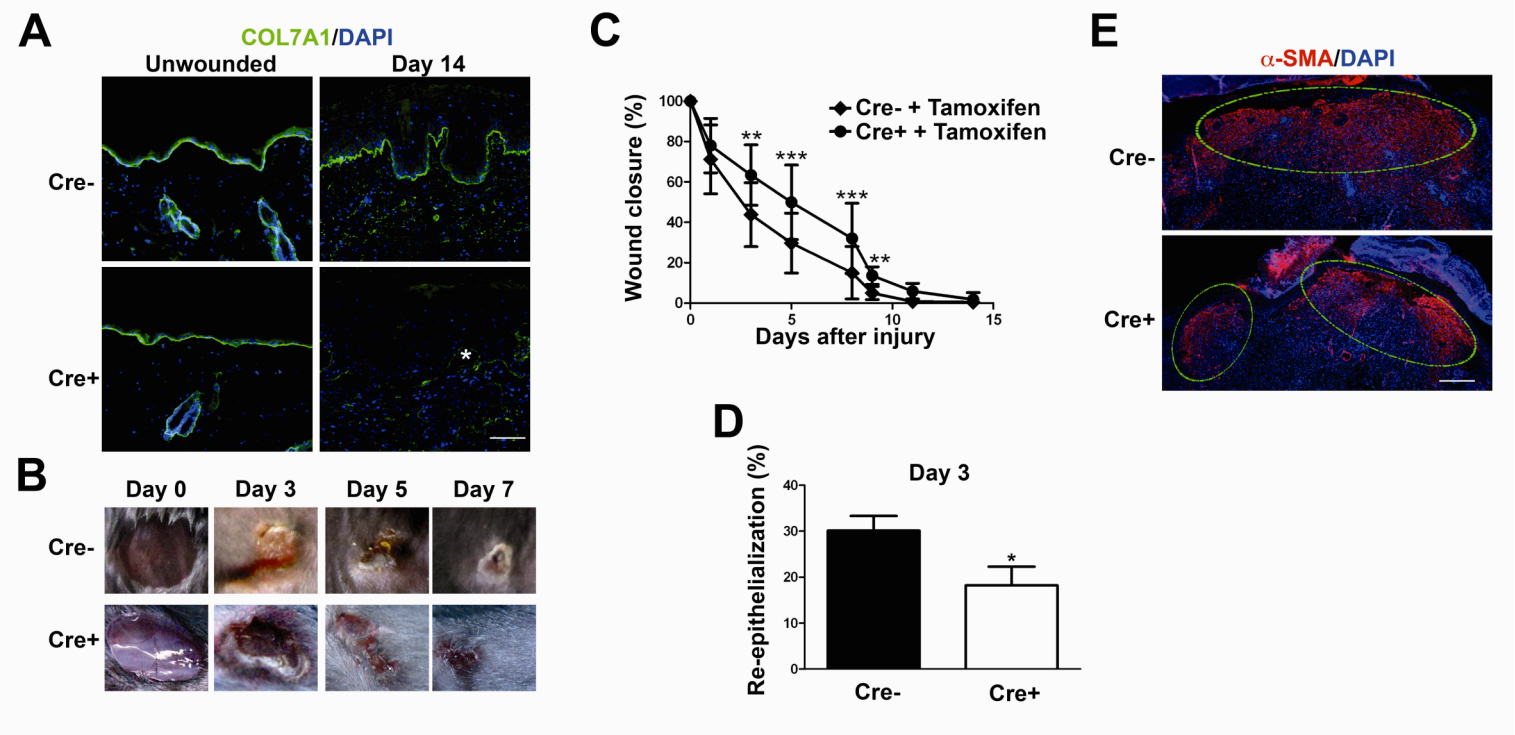

Supplemental Figure 5. Wound healing in the inducible *Col7a1* knockout mouse replicates the findings in the *Col7a1*-hypomorphic mice. **A**, COL7A1 staining (green) confirms loss of COL7A1 in wounds after tamoxifen treatment. Note that the lapsed time, 14 days after tamoxifen treatment is not sufficient to significantly impact the COL7A1 protein content of unwounded skin owing to the high stability of COL7A1. Nuclei were stained with DAPI (blue). Bar = 50 μm. **B**, Mice were wounded on the back with a 6 mm punch biopsy tool, and the healing was documented over 7 days. **C**, Quantification with Image J of the gross wound healing over 14 days shows that loss of COL7A1 significantly delays wound closure between days 3 and 9, n ≥ 27 wounds, values represent mean ± S.E.M. **p<0.01, ***p <0.001 **D**, Quantification of percent re-epithelialization 3 days after wounding, n ≥ 5 wounds, values represent mean ± S.E.M, *p<0.05. **E**, Similar to the *Col7a1*-hypomorphic mice, the myofibroblast maturation is delayed after forced *Col7a1* deletion. Wounds at day 7 were stained for α-SMA (red) and counterstained with DAPI to visualize nuclei, the dense myofibroblast regions are encircled; bar = 200 μm.

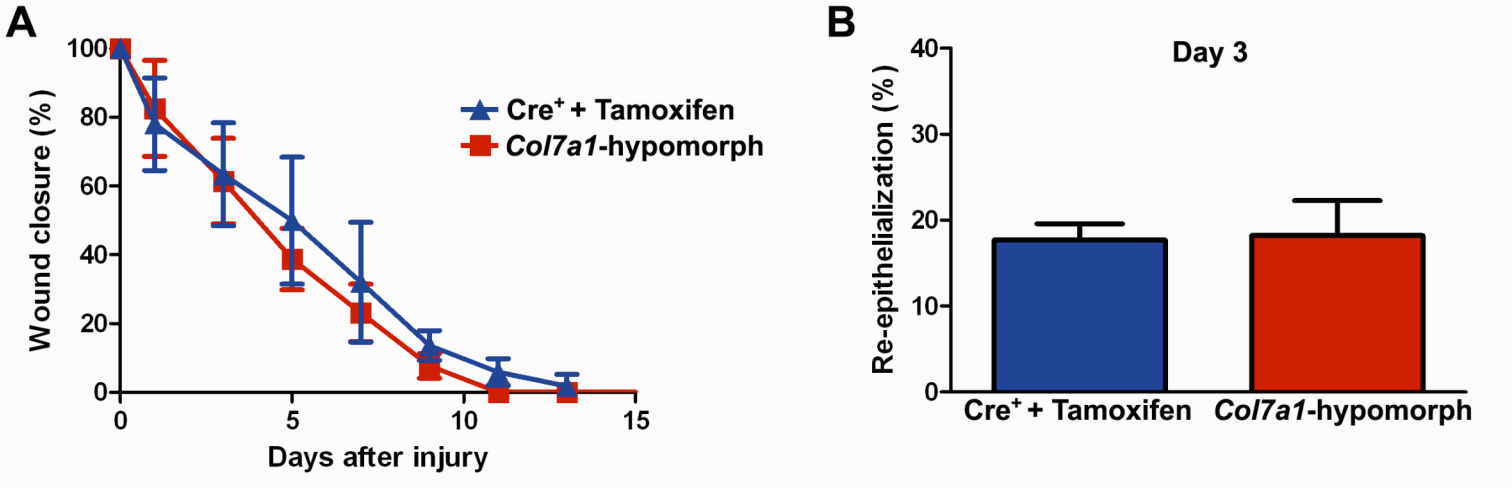

Supplemental Figure 6. Full-thickness wounds heal with similar kinetics in both COL7A1-deficient mouse models. Data from wound closure studies in *Col7a1*-hypomorphic and tamoxifen-treated Cre^+ inducible *Col7a1* knockout mice presented in Figures 1,2 and Supplemental Figure S5 were plotted in the same graphs to visualize differences in healing. The plots showed no significant difference in gross wound healing of full-thickness wounds (**A**) (values represent mean ± S.D) or re-epithelialization of 3-day-old wounds (**B**) (values represent mean ± S.E.M).

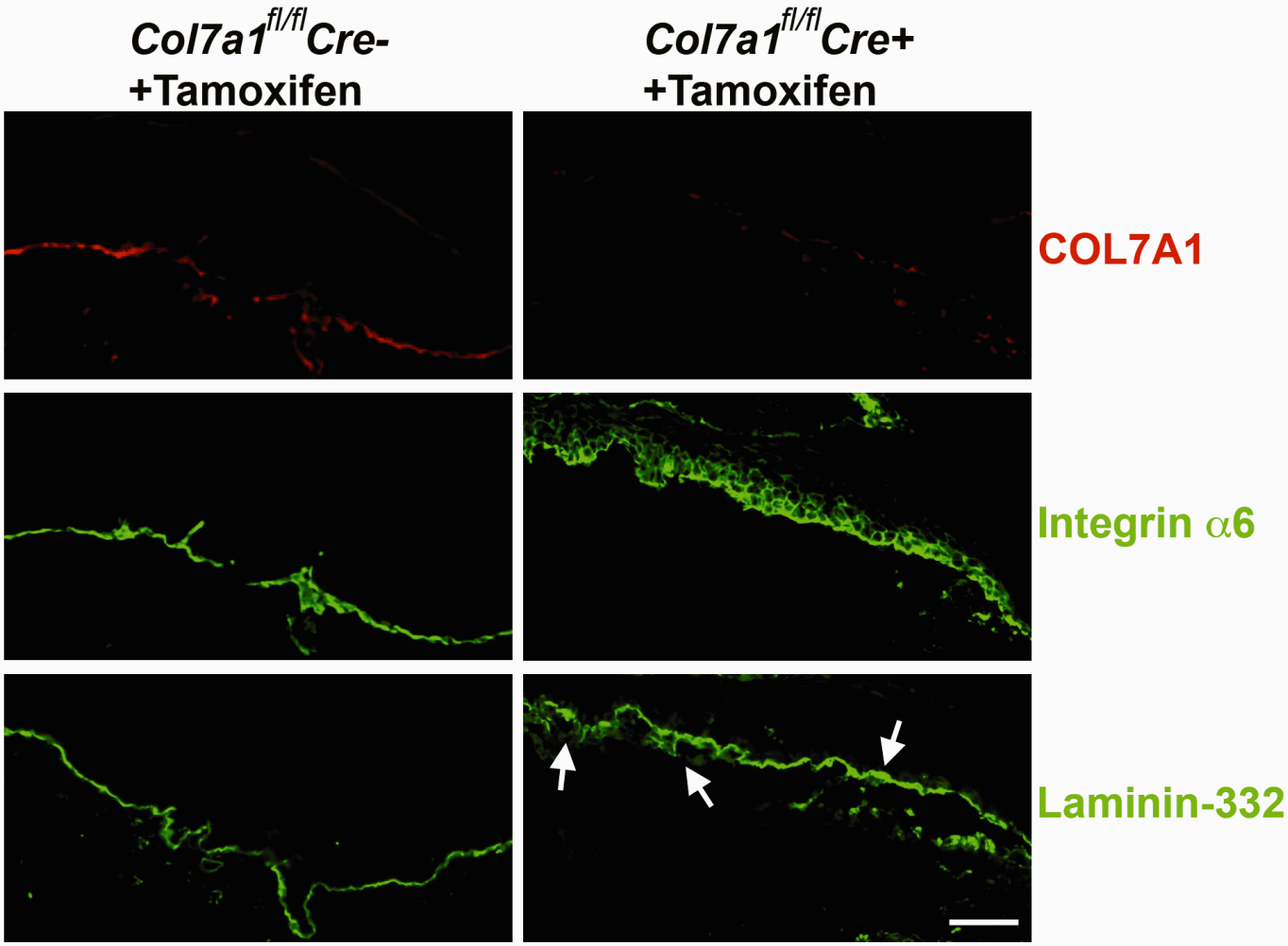

Supplemental Figure 7. Wounds after tamoxifen-initiated *Col7a1* deletion display altered epidermal integrin α6 expression. At day 7, wounds from Cre negative or Cre expressing *Col7a1*$^{fl/fl}$ mice treated with tamoxifen were stained for COL7A1 (red), integrin α6 (green) and laminin-332 (green) as indicated in the figure. In the *Col7a1*-deleted wounds the staining pattern of the integrin α6 subunit in the epidermis is disorganized and not restricted to the basal cell layer. Further, the laminin-332 deposition is also disorganized (white arrows). Thus, wounds where *Col7a1* has been specifically deleted replicate the findings in *Col7a1*-hypomorphic mice; bar = 50 μm. Images were obtained of areas close to the middle of the wound that had undergone re-epithelialization.

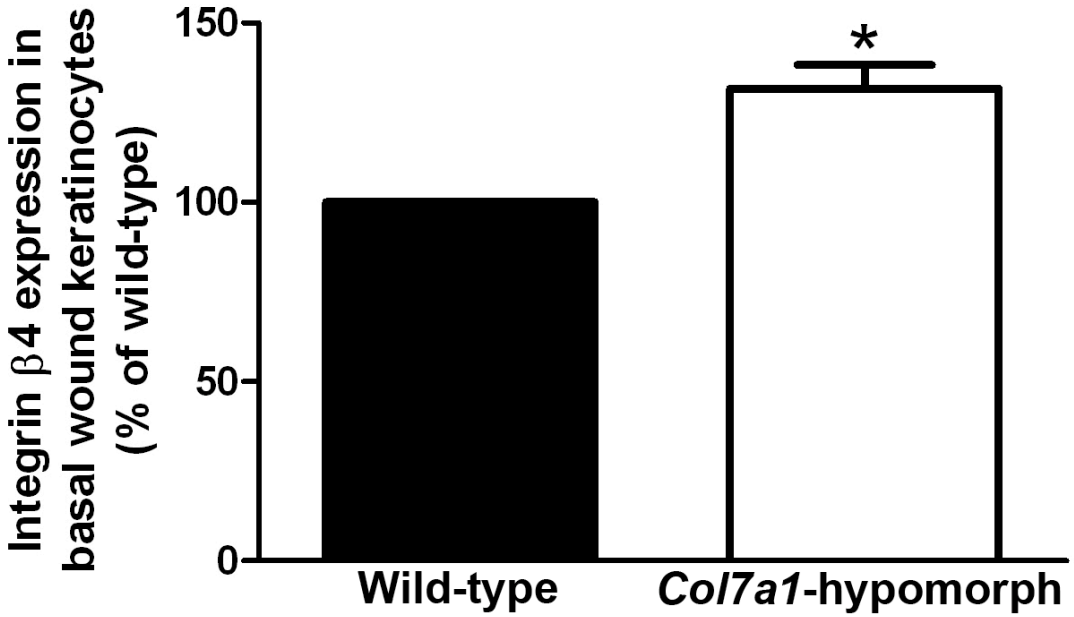

Supplemental Figure 8. Integrin β4-subunit expression is increased in basal keratinocytes in *Col7a1*-hypomorphic wounds. Sections of 7-day-old wounds from wild-type and *Col7a1*-hypomorphic mice were stained for integrin β4 as in Figure 4; photos were taken at the same exposure time and the intensity of integrin β4 staining in basal wound keratinocytes was quantified with Image J. The quantification revealed a slight but significant increase in integrin β4 expression in *Col7a1*-hypomorphic wounds. Values are paired and expressed as the percentage integrin β4 expression of wild-type wounds represent mean ± S.E.M. *$p<0.05$; n = 3 wounds per group.

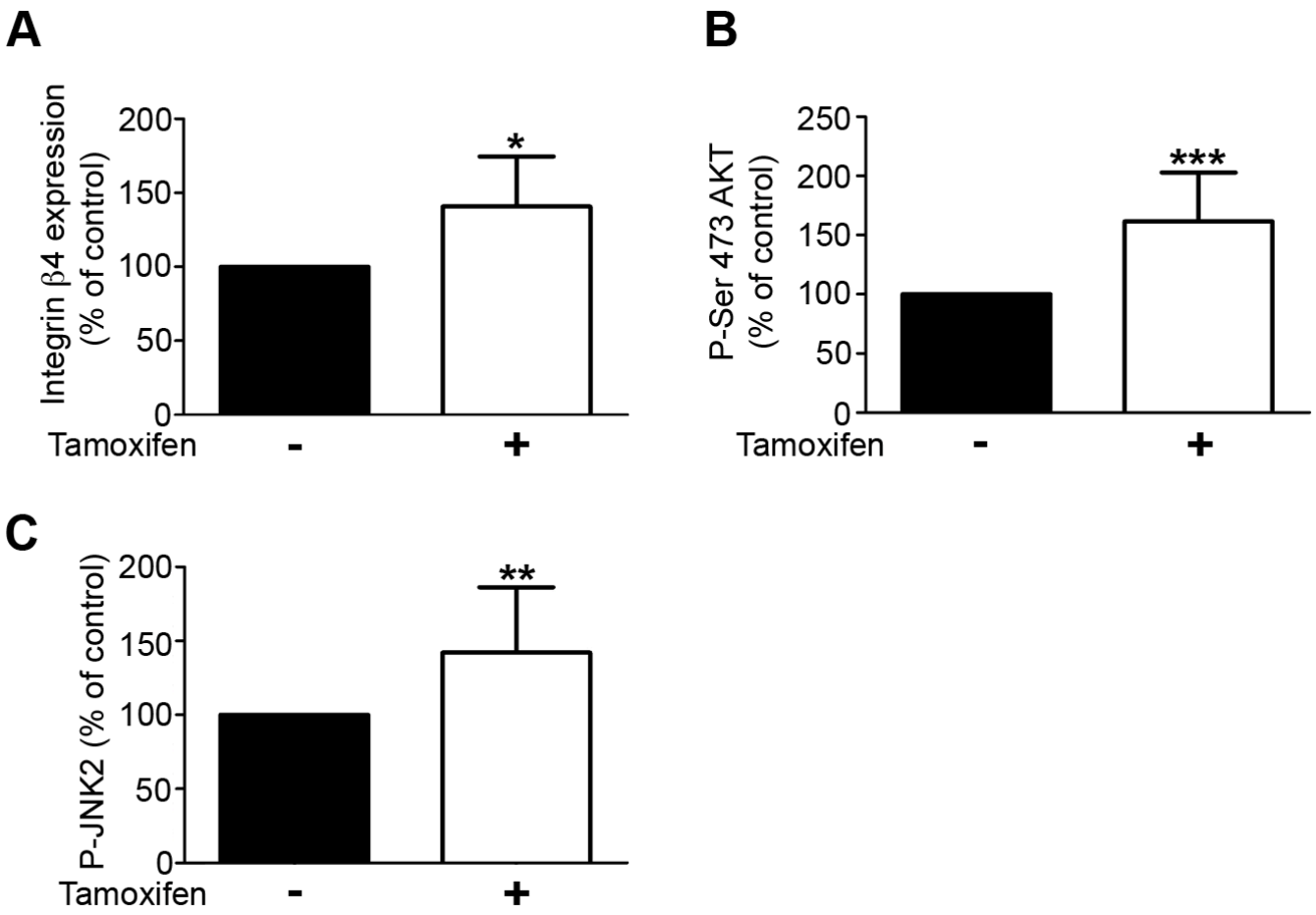

Supplemental Figure 9. Forced COL7A1 loss in keratinocytes results in increased integrin β4 expression, and JNK and AKT activation. Western blots as in Figure 5E were densitometrically quantified using image J. This revealed a significantly increased integrin β4 expression, AKT phosphorylation and JNK2 phosphorylation in keratinocytes isolated from Cre^+ tamoxifen-inducible *Col7a1* knockout mice that had been treated repeatedly with tamoxifen in vitro, n ≥ 3. Values are paired and represent mean ± S.E.M and are expressed as the percentage expression in keratinocytes without tamoxifen; *p<0.05, **p<0.01, ***p<0.001.

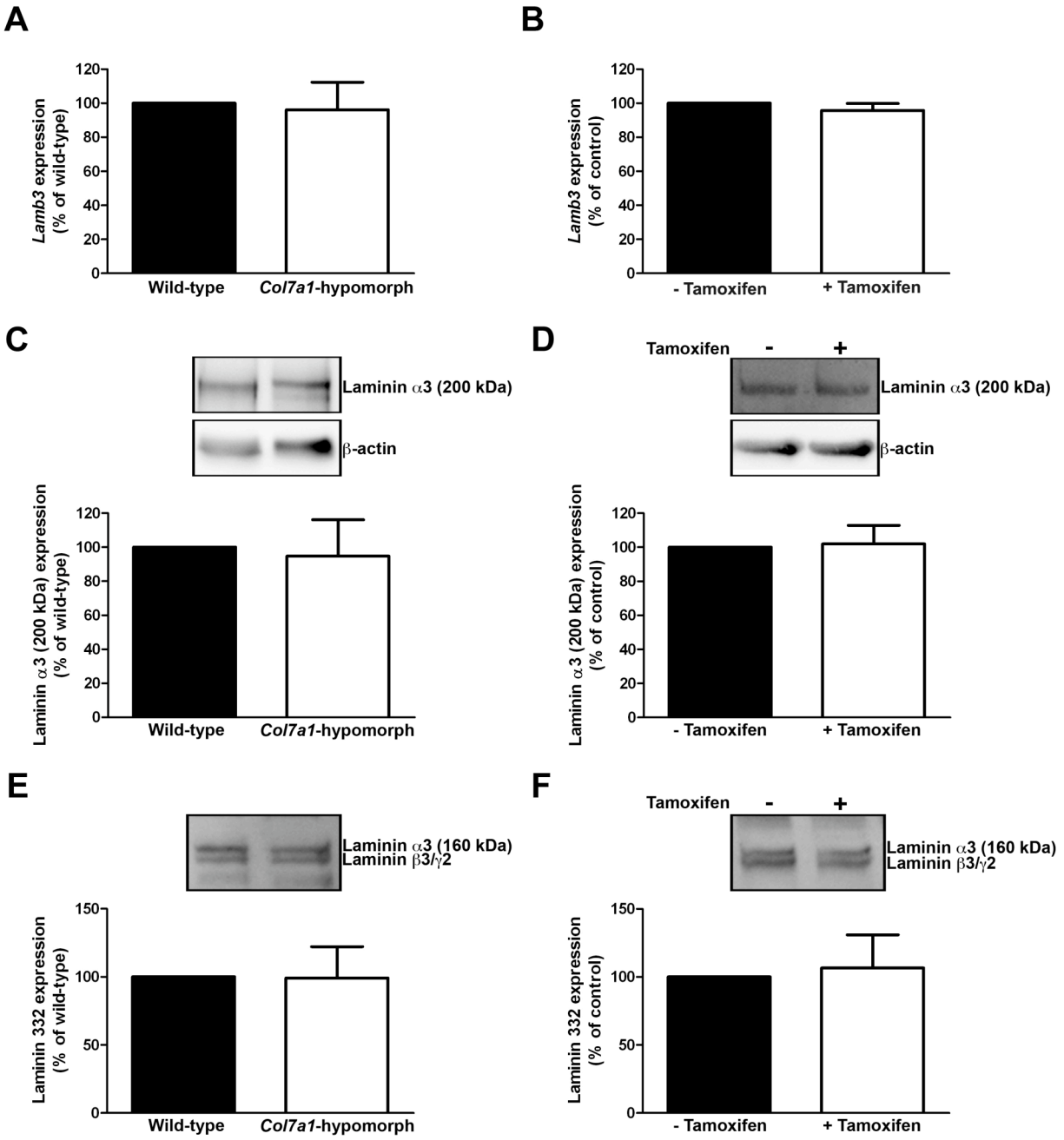

Supplemental Figure 10. Loss of COL7A1 does not alter laminin-332 expression in keratinocytes. The left panels **A, C** and **E**, show experiments with wild-type and COL7A1-hypomorphic keratinocytes, and the right panels **B, D** and **F**, experiments with keratinocytes isolated from Cre^+ tamoxifen-inducible *Col7a1*knockout mice and treated with tamoxifen (+) or DMSO (-). **A, B,** quantitative real-time PCR of *Lamb3* expression. *Gapdh* was used as reference gene. *Lamb3* codes for the laminin β3 chain, which, is only present in laminin-332 (56). Thus, the PCR data are a direct indication of laminin-332 expression. **C** and **D,** Western blots of keratinocyte and matrix lysates probed for laminin-332 and β-actin. Shown is the unprocessed 200 kDa laminin α3 chain. Below are bar graphs of densitometric quantification of multiple blots as above with laminin α3 (200 kDa form) expression normalized to β-actin. In cultured keratinocytes the α3-chain is rapidly processed after secretion to a 160 kDa form. Consequently, the amount of unprocessed α3 chain can serve as a snapshot of the current laminin-332 production by the cells. **E** and **F,** Keratinocyte medium conditioned for 2 days were precipitated with ammonium sulfate, and analyzed by Western blotting. Presented are bands corresponding the processed laminin α3 chain (160 kDa) and to the laminin β3 and γ2 chains. Below are bar graphs of densitometric quantification of multiple blots as above. All values are paired and represent mean ± SEM and are expressed as the percentage expression of wild-type or tamoxifen untreated keratinocyte.

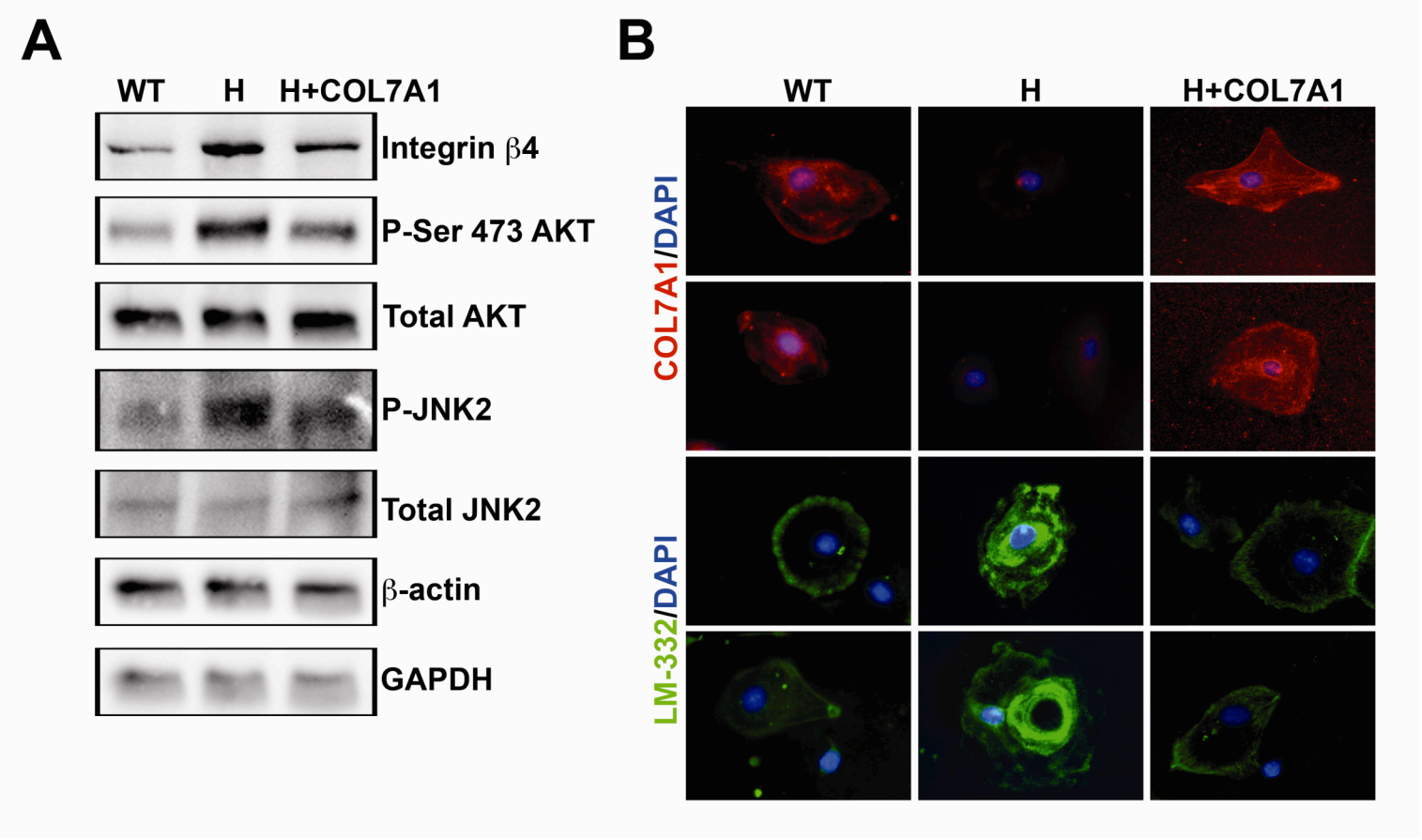

Supplemental Figure 11. Exogenous COL7A1 leads to normalization of integrin β4 expression and JNK and AKT signaling in COL7A1-deficient keratinocytes through normalized laminin-332 deposition. **A,** Western blots of a representative experiment. Wild-type and *Col7a1*-hypomophic keratinocytes (H) were seeded onto 12-well plate wells, which had or had not been coated with 15 μg/ml recombinant COL7A1. The cells were cultured to subconfluence in the presence of ascorbic acid for 2 days, then lysed and subjected to Western blot analysis. In *Col7a1*-hypomophic keratinocytes, culture on recombinant COL7A1 reduced integrin β4 expression, AKT phosphorylation (P-Ser 473 AKT) and JNK2 (P-JNK2) phosphorylation, as compared to culture on plastic. Total AKT, JNK-2, β-actin and GAPDH are shown as loading controls. **B**, immunofluorescence staining of wild-type and *Col7a1*-hypomophic keratinocytes (H) grown on coverslips, which were or were not coated with recombinant COL7A1, under the same conditions as described in **A**. The cells were stained for COL7A1 (red) and LM-332 (green), and the nuclei were visualized with DAPI (blue). COL7A1 is largely absent from *Col7a1*-hypomorphic keratinocytes, whereas it is clearly detectable around *Col7a1*-hypomorphic cells seeded on COL7A1-coating. Importantly, recombinant COL7A1 restored the abnormal LM-332 organization seen in COL7A1-deficient keratinocytes.

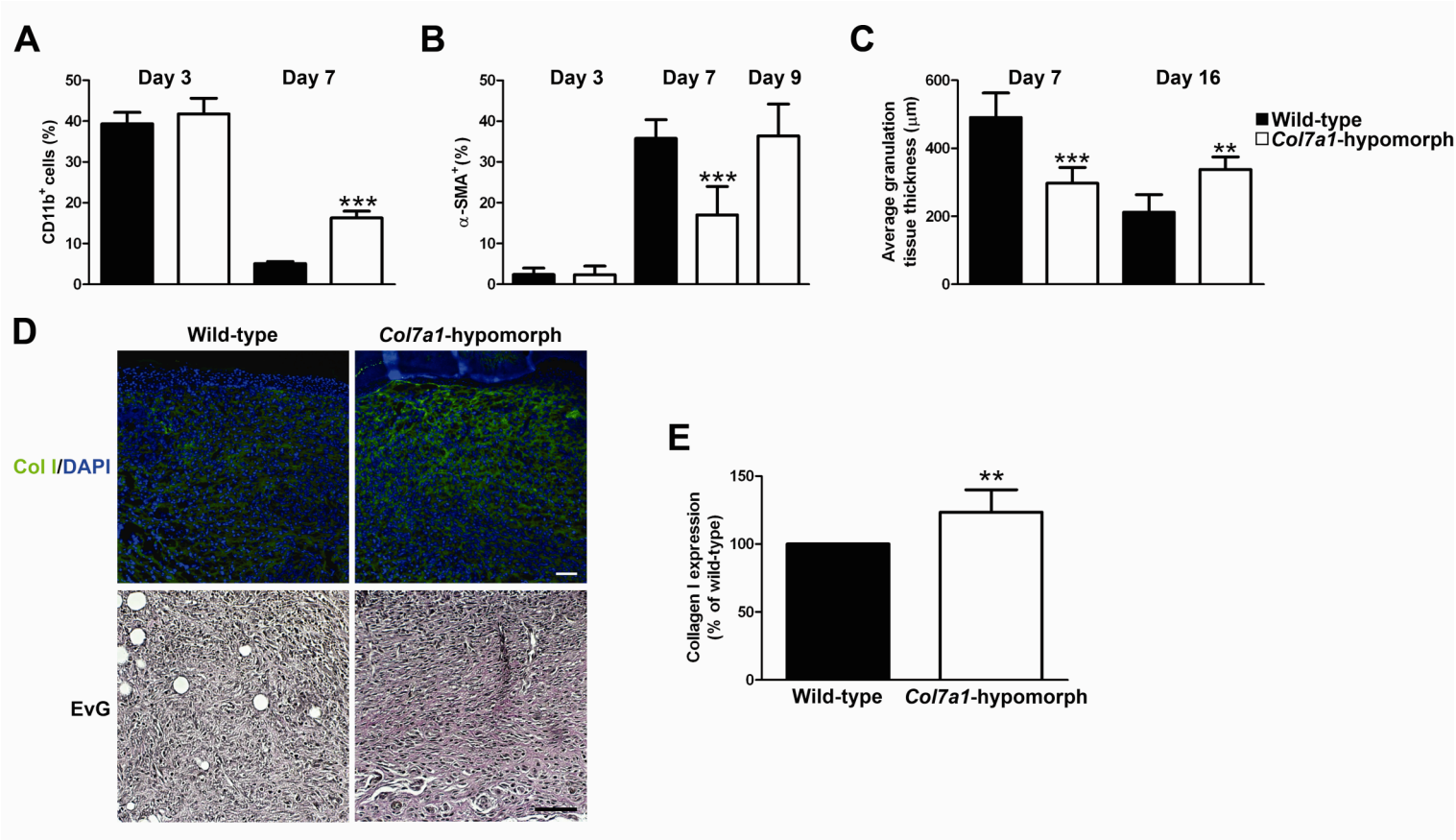

Supplemental Figure 12. COL7A1-deficiency leads to abnormal granulation tissue formation. **A**, Quantification of CD11b$^+$ positive cells as in Figure 6 in 3- and 7-day-old wild-type and COL7A1-deficient wounds. The results are expressed as the percentage of total cells in granulation tissue. The analyses revealed significantly more CD11b$^+$ inflammatory cells in *Col7a1*-hypomorphic wounds than in wild-type wounds 7 days after wounding. **B,** α-SMA staining as in Figure 6 in 3-, 7- and 9-day-old wounds. Determination of the α-SMA positive area revealed a significant reduction in α-SMA positive myofibroblasts in 7-day-old *Col7a1*-hypomorphic wounds. This had recovered by 9 days after wounding. **C,** The thickness of the granulation tissue shown by H&E staining as in Figure 2C was measured. The granulation tissue development was significantly delayed in COL7A1-deficent wounds at day 7 and in the resolution stage at day 16. **D,** Collagen I is significantly increased in COL7A1-deficient granulation tissue. Collagen expression in 7-day-old wild-type and *Col7a1*-hypomorphic wounds was assessed by immunofluorescence staining with collagen I antibodies (upper panel) and Elastica van Gieson (EvG) staining (lower panel). ColI (green), collagen I; DAPI (blue) stains nuclei. Bars = 50 μm. **E,** Quantification of the intensity of the immunofluorescence staining shown in panel **D**. Collagen I is significantly increased in COL7A1-deficient granulation tissue. The values are paired and expressed as the percentage collagen I staining of wild-type wounds. Image J was used for all quantification in the figure. N ≥ 3, values represent mean ± S.E.M. **p<0.01, ***p<0.001.

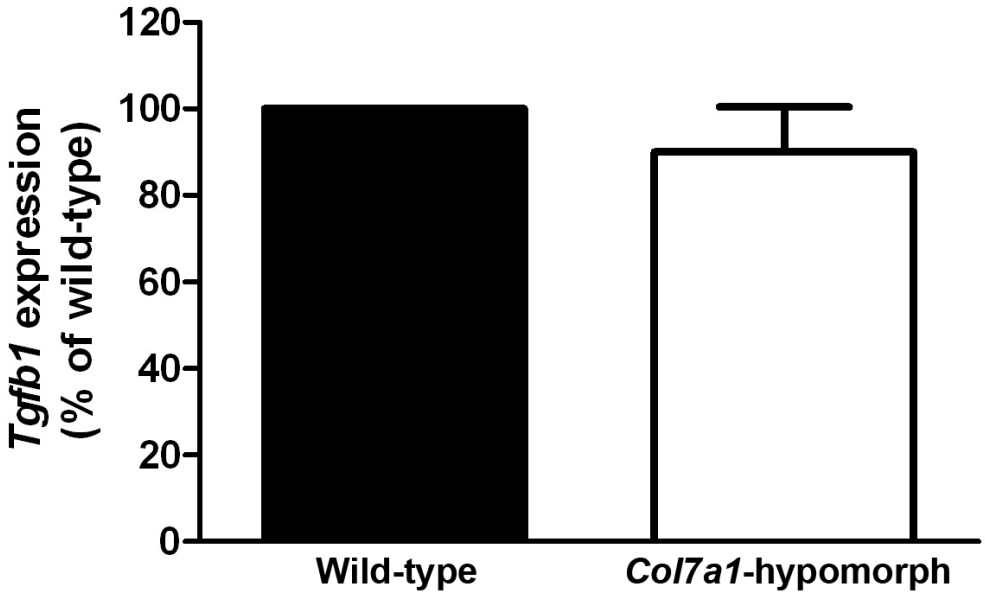

Supplemental Figure 13. Loss of COL7A1 does not alter TGF-β expression in keratinocytes. Subconfluent wild-type and *Col7a1*-hypomorphic keratinocytes were analyzed for *Tgfb1* expression by quantitative real-time PCR. *Gapdh* was used as reference gene. No significant difference in *Tgfb1* expression was observed. Values are paired and expressed as the percentage of wild-type keratinocyte expression and represent mean ± S.E.M, n = 3.